Journal of Materials Chemistry

Dynamic Article Links

Cite this: J. Mater. Chem., 2012, 22, 21749

www.rsc.org/materials

PAPER

Energy coupling processes in InGaN/GaN nanopillar light emitting diodes embedded with Ag and Ag/SiO_2 nanoparticles

Lee-Woon Jang,[a] Dae-Woo Jeon,[a] Trilochan Sahoo,[a] Alexander Y. Polyakov,[a] Balasubramaniam Saravanakumar,[a] Yeon-Tae Yu,[a] Yong-Hoon Cho,[b] Jin-Kyu Yang[c] and In-Hwan Lee*[a]

Received 12th June 2012, Accepted 31st August 2012
DOI: 10.1039/c2jm33759b

We synthesized Ag and Ag/SiO_2 nanoparticles (NPs) and investigated the energy coupling processes between the localized surface plasmons of NPs and the active quantum well regions of nanopillar light-emitting diodes (LEDs). Nanopillar LEDs embedded with Ag NPs exhibited a decreased photoluminescence (PL) intensity, while the PL was markedly enhanced for Ag/SiO_2 NP embedded nanopillar LEDs. Though the PL decay times decreased in both cases compared to the sample without NPs, the difference in observed optical behavior suggests that different types of energy coupling (EC) are involved.

Introduction

Surface plasmons (SPs) are quasi-particles formed at the metal–dielectric interface due to collective oscillation of conduction electrons.[1] Metal nanostructures are used to create localized surface plasmons (LSPs)[2] that are of great interest because their properties can be tuned to enhance light produced in the dielectric (or light emitting medium) and to provide good phase matching of electromagnetic radiation emitted in the dielectric and response function of the LSP system. These LSPs have been studied for applications in sensing, medical imaging, and surface enhanced spectroscopy.[3–6] Recently, the LSP phenomena have attracted great interest in InGaN/GaN based light-emitting diodes (LEDs) as the luminescence efficiency can be improved by the energy coupling (EC) of LSPs with the active quantum well (QW) region of such LEDs.[7] According to the EC mechanism, when the metal nanostructure forming LSPs were deposited in close proximity to the active layer of LEDs and when the emission energy matches the LSP oscillation energy, excitons in the active layer of LEDs can transfer their energy directly to the LSP mode as well as emitting light at the active layer, rather than decay *via* radiative and non-radiative recombination channels in the semiconductor structure. In other words, the internal quantum efficiency (η_{int}) of the LEDs is improved due to coupling with LSPs of the metal nanostructure and is given by $\eta_{int} = (k_{rad} + k_{LSP})/(k_{rad} + k_{non} + k_{LSP})$ so that optical properties can be greatly improved due to the operation of the k_{LSP} term, where k_{rad} and k_{non} are the radiative and non-radiative recombination rates of electron–hole pairs and k_{LSP} is the coupling rate between the active layer and LSPs.[7] The modification of the optical properties by LSP coupling depends on the EC rates and it is related to the LSP energy and spacer thickness between the metal nanostructure and the active layer.[3,7,8] The LSP energy is controlled by changing the shape and size of metal nanoparticles (NPs).[9,10] In previous reports the metal thin film was deposited on the surface by an e-beam evaporator and then an annealing process was performed to form the metal nanostructure.[10–12] However, these NPs were subject to metal oxidation and diffusion into the GaN layer leading to performance degradation.[13,14] These considerations make it important to better understand the stability and contamination issues of the metal nanostructure produced by alternative methods and to study the characteristics of LSPs associated with such alternative structures.

Recently, we reported on the properties of chemically synthesized Ag and Ag/SiO_2 NPs and the performance enhancement of LEDs coated with these NPs.[15,16] The attractive feature of such NPs is the possibility to increase and carefully regulate the NP density with consequent increase in the enhancement factor. This is in contrast to metal NPs formed by annealing. Moreover, for core–shell Ag/SiO_2 NPs a very substantial improvement in performance stability was observed as compared to pure metal NPs.[17] This makes the chemical synthesis a potentially very promising technology for design and optimization of LSP enhanced LEDs and related applications.

However, the thickness of the spacer layer between the active region of LED and the LSP region is still a serious concern, with the thickness of the p-GaN emitter layer in contemporary LEDs more or less fixed by the spreading resistance and junction performance considerations and difficult to alter.[7,11] The spacer thickness for effective LSP coupling has been already reported, and the effective distance of the Ag nanostructure from the active

[a]*School of Advanced Materials Engineering and Research Center of Advanced Materials Development, Chonbuk National University, Jeonju 561-756, Korea. E-mail: ihlee@jbnu.ac.kr; Fax: +81-63-270-2305; Tel: + 82-63-270-2290*
[b]*Department of Physics, KAIST, Daejeon 305-701, Korea*
[c]*Department of Optical Engineering, Kongju National University, Kongju, Chungnam 314-701, Korea*

layer of LEDs should be within several tens of nanometers. However, in conventional blue LED structures the thickness of the p-type GaN spacer layer is generally greater than 76 nm in order to form a well-behaved p–n junction and to provide reasonably low spreading resistance. Such a GaN thickness is too large for the effective LSP coupling process.

As a solution to the problem posed by the high thickness of n-GaN and p-GaN layers of conventional LEDs, we proposed the fabrication of NPs embedded in InGaN/GaN based nanopillar LEDs. In such architecture the NPs could be placed very close to the active layer of the nanopillar LEDs and one can expect effective interaction between them. In what follows we analyze the optical properties of the Ag and Ag/SiO_2 NP embedded nanopillar LEDs and describe the main factors determining the efficiency of the energy coupling process for Ag and Ag/SiO_2 NPs.

Results and discussion

SP and LSP are propagating excitations of charge density waves and their presence can strongly influence the fluorescent emission of nearby molecules or emission source in conjunction with electromagnetic fields near the metal surface.[3,6–11] These electromagnetic fields depend on the separation between individual NPs, their size and geometry,[9,18] but first and foremost, on the distance from the metal surface.[3,8] In ref. 15, we analyzed the LSP resonance characteristics of such NPs and reported that the electromagnetic field is strongly confined near the surface and exponentially decays in GaN. Consequently, the LSP resonance of NPs is substantially different from the metal film[7] and it has been theoretically demonstrated that fluorescence of samples with NPs is greatly affected by the distance of the NP layer from the light emitting layer and between NPs.[3,16,19] In our structure, the SiO_2 shell increases the distance from the metal surface and leads to a relatively low enhancement, but it can provide the stability and uniformity of metal NPs[8] and prevent parasitic energy losses.[3,6,20] Moreover, Ag/SiO_2 NPs are expected to suppress electrical shorting in nanopillar LEDs.

Based on these considerations, we prepared Ag and Ag/SiO_2 NP embedded nanopillar LEDs to investigate the EC processes. The morphology of the Ag and Ag/SiO_2 NPs was investigated by TEM measurements (see Fig. 1(b) and (c)). It can be seen that both the Ag and the Ag/SiO_2 NPs were mostly spherical and the Ag NPs were completely covered by the SiO_2 shell of nearly uniform thickness. The estimated size of Ag NPs was 30–80 nm while that of the Ag/SiO_2 NPs was 50–80 nm with the SiO_2 shell of 20 nm. The selected-area electron diffraction (SAED) pattern of Ag and Ag/SiO_2 NPs confirmed the presence of the crystalline Ag core.[21] However, the non-uniform size distribution of the Ag NPs resulted in absorption spectra broadening.[22] For Ag/SiO_2 core–shell NPs, the presence of the silica shell with refractive index higher than air is expected to shift the peak in plasma reflection/absorption spectra to a longer wavelength, as predicted by Mie theory (see *e.g.* ref. 23–25) and as demonstrated for Au/SiO_2 NPs in ref. 8. Such red shift in comparison with Ag NPs has indeed been observed in our earlier papers (ref. 15–17). This shift is illustrated in Fig. 1. As is evident from the figure, the Ag NPs show the broad absorbance spectra with peak value at 420 nm while the Ag/SiO_2 NPs show the broad absorbance spectra with peak at 440 nm. One can notice that the absorbance wavelengths of these NPs are in the blue emission region of nanopillar LEDs and therefore these NPs could be suitable for EC by LSP.[12,26]

To study the possible EC mechanism between the NPs and the nanopillar LEDs, the synthesized Ag and Ag/SiO_2 NPs were directly embedded between the nanopillar LEDs by drop casting NP solution. Fig. 2 shows the 3-D sample structure and SEM images of nanopillar LEDs, Ag NP embedded- and Ag/SiO_2 NP embedded nanopillar LEDs, respectively. The images clearly show that the nanopillars have an approximate diameter of 100–200 nm and a length of 500 nm. The distance between nanopillars is around 200 nm. After the Ag and Ag/SiO_2 NP coating in 10 μl colloidal solution, the Ag and Ag/SiO_2 NPs on the top of the p-GaN of nanopillar LEDs were removed by the physical

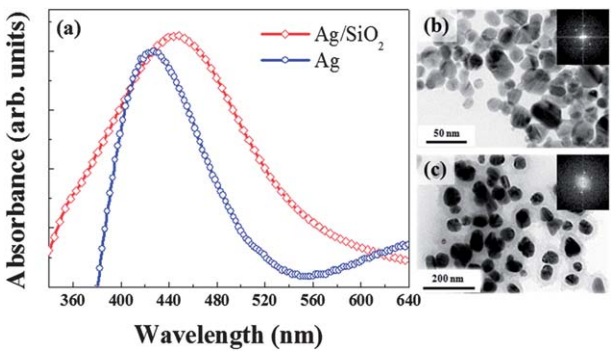

Fig. 1 The absorbance spectra (a) and TEM images (b and c) of the Ag and Ag/SiO_2 NPs synthesized by the sol–gel method. Each TEM inset shows the SAED pattern taken from the Ag core.

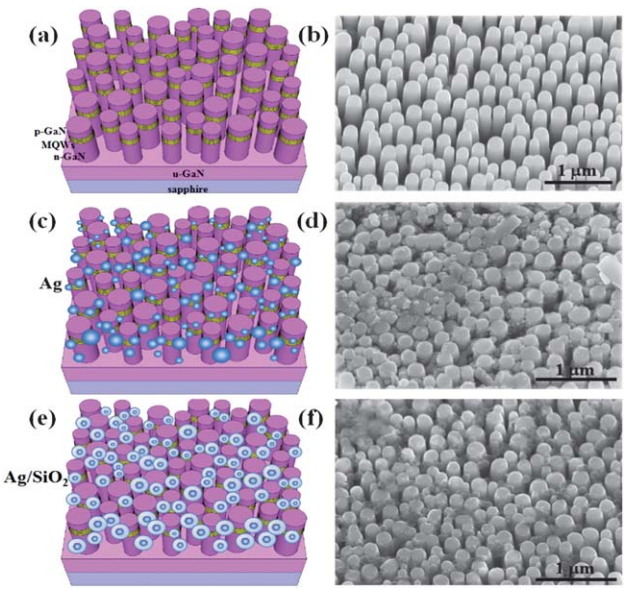

Fig. 2 Schematic sample structure of the nanopillar (a), Ag embedded nanopillar (c), and Ag/SiO_2 NP embedded nanopillar (e). The field emission SEM images taken after Ag and Ag/SiO_2 NP coating are presented (b) for the nanopillar structure, (d) for the Ag embedded nanopillar structure, and (f) for the Ag/SiO_2 NP embedded nanopillar structure. The NPs on the top of nanopillars are clearly removed after the physical stamping process.

stamping technique[27] to avoid the disturbance of the incident laser beam and facilitate the extraction of emitted light. As seen in Fig. 2(d) and (f), the NPs on top of nanopillars were clearly removed after this process and the embedded NPs were close to the active layer of nanopillar LEDs.

The front-side photoluminescence (PL) spectra from the Ag and Ag/SiO_2 NP embedded nanopillar LEDs are shown in Fig. 3. The PL measurements are performed with near normal incidence of the excitation laser beam. The incident laser light with the wavelength of 325 nm virtually does not interact with the NPs (see the spectra in Fig. 1), but effectively excites luminescence in the MQW region of nanopillar LEDs. This luminescence is peaked at 450 nm wavelength and is well tuned to the absorption spectra of NPs. The PL intensity of the Ag embedded sample was found to decrease by 72% while the PL intensity of the Ag/SiO_2 embedded sample was increased by 59% relative to the nanopillar LEDs. In order to perceive these intensity changes, it is necessary to understand the EC process of NP embedded nanopillars. Usually, EC to the non-radiative recombination process in the emitter is confined to the distance of several tens of nanometers.[28]

However, within the order of sub-10 nm, a dipole–dipole interaction is more important than for distances of >10 nm and it can proceed *via* different EC mechanisms, such as Förster or Dexter transfer.[28,29] Unfortunately, the probability of these transitions is usually low[28] and one has also to consider consequences of ohmic losses and fluorescence quenching.[28–32]

In the case of Ag NPs, the Ag cores were capped by several nanometers of cetyl trimethyl ammonium bromide (CTAB) during synthesis by the sol–gel method. The CTAB can provide a stable formation and prevent the aggregation of Ag NPs.[33] However it cannot prevent the electron tunnelling from the active layer and between individual NPs. This would create an energy leak between the active layer and Ag NPs for Ag NP embedded nanopillar LEDs.[17,29,34]

Such additional loss mechanisms could perhaps account for the decreased PL intensity of the Ag NP embedded sample.

In the case of Ag/SiO_2 NPs, the Ag sphere was capped by a 20 nm SiO_2 shell. The SiO_2 provides a large potential barrier and it can prevent the tunneling of electrons. Contrary to the Ag NP embedded sample, the PL intensity of Ag/SiO_2 NP embedded nanopillar LEDs was increased. This suggests that the Ag/SiO_2 NPs can prevent the energy loss of LSP thus producing the enhancement of luminescence efficiency.[3,8,31,35] The results of theoretical simulation and experimental studies[15–17] indicate that the interspacing distance between the Ag and the active layer in the case of the Ag/SiO_2 NP embedded sample should be sufficient to achieve the LSP coupling.

For more specific analysis, we investigated the PL decay profiles of our samples by time-resolved PL (TRPL) measurements. Fig. 4 shows the PL decay curves for the three studied nanopillar structures. The decay curves can be deconvoluted into fast decay and slow decay components, with the fast decay often believed to be due to excitonic relaxation combined with non-radiative relaxation.[11,12] This fast PL decay time of nanopillar LEDs at the peak emission wavelength ($\lambda = 450$ nm) was 4.32 ns, and the characteristic decay times of Ag and Ag/SiO_2 embedded samples were 1.5 ns and 3.86 ns, respectively.[36] From these transient PL results the EC efficiency for each sample could be calculated using eqn (1):

$$\eta_{EC} = k_{EC}/(k_{EC} + k_{NP}), \quad (1)$$

here, k_{NP} represents the decay time of nanopillar LEDs, and k_{EC} represents the decay time of NP embedded nanopillar LEDs. The EC efficiency for Ag NPs was calculated to be 74.2%, while the EC efficiency for Ag/SiO_2 NPs was estimated to be 52.8%. The higher EC efficiency of Ag NP embedded nanopillar LEDs is due to the smaller interspacing distance.[16,29,35] However, due to tunneling between individual NPs and related parasitic energy dissipation mechanisms for nanopillar LEDs with close-set Ag NPs,[30–32] the net result is quenching of PL efficiency by Ag NPs rather than enhancement of PL efficiency (see ref. 15–17). The observed decrease of PL intensity for the corresponding sample was 72%.

In contrast, the Ag/SiO_2 NP embedded nanopillar LEDs show a lower EC efficiency than Ag NPs due to the SiO_2 shell and hence the larger separation of Ag NPs from the active layer and between Ag NPs.[16,31] Nevertheless, the PL intensity was increased compared to the Ag embedded sample and enhanced PL efficiency is consistent with the EC efficiency of 52.8%.

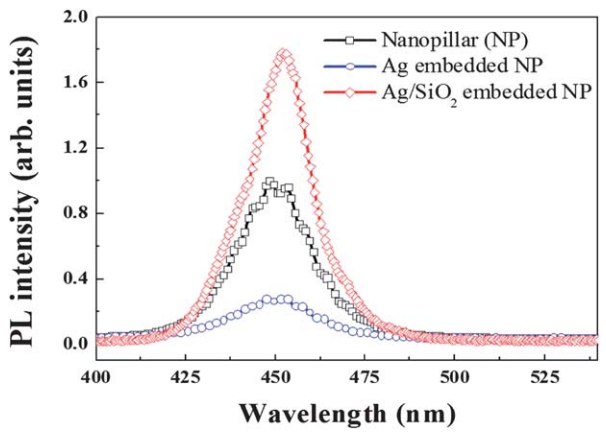

Fig. 3 Room temperature PL spectra from the nanopillar, Ag NP and the Ag/SiO_2 NP embedded sample.

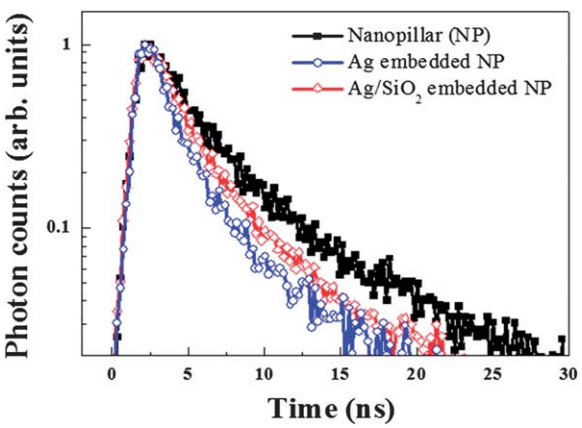

Fig. 4 Time-resolved photoluminescence decay curves from the nanopillar, Ag NP embedded nanopillar (blue), and Ag/SiO_2 NP embedded nanopillar (red) at room temperature.

Therefore, we observe that there exists a correlation between the EC efficiency, between the nanopillar LEDs and NPs, the PL intensity and effective TRPL decay time. The qualitative difference between the results of Ag NPs (decrease of PL intensity) and the Ag/SiO_2 NPs (increased PL intensity) most likely comes from the quantum mechanical tunneling processes in Ag NPs resulting in the EC energy being converted into non-radiative losses rather than into enhanced excitons output.

It should be noted that a very reasonable agreement between the experiment and simple estimates based on eqn (1) is a bit surprising. Indeed, the general treatment discussed above is an oversimplification. It assumes that the geometry is the same as in standard modeling in which the LSP is above the MQW region and the emitted light propagates upwards from the NP surface into the air. The actual situation in the case in hand is very different: the NPs are located laterally to the MQW region and the light emitted by NPs has to escape the etched "well" surrounding the nanopillar. Theoretical modeling suggests that the fringe electric field of the LSP penetrates into GaN only down to about 20 nm.[15] Hence, only 20 nm ring of the ~100 nm diameter in the MQW region of the nanopillar should be affected by the LSP enhancement, *i.e.* the "effective" "activated" region volume should be only about 64% of the total volume of the nanopillar. Then, only photons emitted from the nanopillars at angles lower than critical (approximately arcctg [(p-GaN + MQW thickness)/(distance between nanopillars)]) can leave the LSP region unhindered if one does not consider scattering on NPs. Finally, only the near-surface region of the nanopillars should have the recombination decay time strongly affected by emission into LSP states. The effective lifetime measured in the experiment should be the sum of reciprocal bulk and sub-surface recombination lifetime. These considerations suggest that the amount of intensity increase and lifetime decrease due to interaction with LSPs should be much higher than suggested by the simple estimates above. Clearly, more refined modeling taking into account all the enumerated factors is necessary, but the task is rather complicated. Development of such a model is currently underway in our laboratories.

Experimental methods

The InGaN/GaN multi-quantum-well (MQW) epitaxial structure was grown by the metal organic chemical vapor deposition technique. Trimethylgallium, trimethylindium and NH_3 were used as precursors for Ga, In and N, respectively. A thermal annealing of the *c*-plane sapphire substrate was carried out at 1100 °C for 10 min, followed by the growth of a low temperature GaN buffer layer. A 1 μm-thick undoped GaN layer and a 2 μm-thick n-type GaN layer were grown at 1060 °C. Then, five pairs of InGaN/GaN MQW were grown on high quality GaN epitaxial layers. The GaN barriers and InGaN wells were grown at temperatures of 850 °C and 750 °C, respectively. A 150 nm thick p-type GaN layer was grown on top.

In order to fabricate the nanopillar LEDs, a 100 nm-thick SiO_2 and 15 nm-thick Ni as a mask were deposited on the surface by plasma-enhanced chemical vapour deposition and an e-beam evaporator, respectively. The sample was subsequently annealed under flowing N_2 at temperature of 800 °C for 1 min to form the Ni clusters. Finally, the SiO_2 and GaN layers were etched using an inductive-coupled-plasma-reactive ion etching (ICP-RIE) system. The etch depth from the GaN surface was approximately 500 nm. After completing the ICP-RIE process, the sample was dipped in buffer oxide etchant to remove the Ni clusters and the SiO_2 layer on the surface.[37] This physical etching process by ICP-RIE using SiO_2 and Ni mask provided a simple technique for fabricating a nanopillar structure with uniformly etched region. However, it induces the structural defects due to ion bombardment during etching and these defects act as non-radiative recombination centers. In order to minimize the ICP damage,[38] the nanopillar LEDs were annealed by rapid thermal annealing at 800 °C for 1 min under nitrogen ambient.

To synthesize the Ag and SiO_2 capped Ag NPs, analytical grade tetraethyl-orthosilicate and silver nitrate hydroxide were used. De-ionized water was used in all processes. A typical preparation procedure was performed as follows:[39] a 500 mL beaker was filled with 180 mL of aqueous solution of CTAB (0.145 g) under vigorous magnetic stirring. Aqueous solution of silver nitrate (0.1 M, 10 mL) was then added to the above solution. 20 mL of aqueous solution of ascorbic acid as reducing agent were added to the solution in 5 min. After the solution was stirred for further 10 min, sodium hydroxide (0.1 M) was added to speed up the reaction and the pH of the solution was about 5. It should be noted that the actual value of pH can play various roles. One of the effects involved is the influence of pH on the density of the surface state of NPs.[40–43] However, in our case the pH value is related to the SiO_2 shell thickness. With increasing pH after the silver colloids process, the SiO_2 shell thickness is increased. We chose pH equal to 5 producing a relatively low coating rate because the thin SiO_2 shell is needed for efficient LSP.[44] Subsequently, 50 mL of ethanol and 1 mL of tetraethoxysilane (TEOS) were added into the above-mentioned silver colloids. The solution was stirred for another 3 hours at room temperature (RT).

The morphology of the Ag and Ag/SiO_2 NPs was investigated by high-resolution TEM and SEM. For room temperature PL measurements, the 325 nm line of a He–Cd laser with a 100 μm diameter and a 25 mW power was used as the excitation source. TRPL was performed under pulse excitation by frequency-doubled (398 nm) laser pulses from a Ti:sapphire mode locked laser and the signals were analysed using a streak camera with an overall resolution of 15 ps.

Conclusions

In summary, the distance from the metal surface is the most important factor in obtaining the high EC efficiency. The nanopillar LEDs can provide a minimum interspacing between the active layer and LSP of metal NPs. However, the Ag NP embedded nanopillar LEDs showed the quenched PL intensity because of the losses presumably due to the quasi-continuous character of the close-set Ag NP adjacent to the MQW region of the nanopillar LEDs. Although the SiO_2 shell increases the interspacing between the active layer and LSP of metal and decreases the EC efficiency, it can prevent the electron tunneling and thus produce very markedly enhanced luminescence efficiency of nanopillar LED structures. These considerations make us believe that the Ag/SiO_2 NPs are optimal for stable and reliable LEDs performance enhancement *via* efficient energy

coupling between the LED active regions and the NP related LSPs.

Acknowledgements

This work was supported by the National Research Foundation of Korea (NRF) funded by the Korea government (MEST) (2010-0019626, 2010-0026614).

Notes and references

1 W. L. Barnes, A. Dereux and T. W. Ebbesen, *Nature*, 2003, **424**, 824.
2 K. A. Willets and R. P. Van Duyne, *Annu. Rev. Phys. Chem.*, 2007, **58**, 267–297.
3 A. V. Akimov, A. Mukherjee, C. L. Yu, D. E. Chang, A. S. Zibrov, P. R. Hemmer, H. Park and M. D. Lukin, *Nature*, 2007, **450**, 15.
4 I. K. Ding, J. Zhu, W. Cai, S. J. Moon, N. Cai, P. Wang, S. M. Zakeeruddin, M. Gratzel, M. L. Brongersma and M. D. McGehee, *Adv. Energy Mater.*, 2011, **1**, 52.
5 Y. Yan, C. J. Ochs, G. K. Such, J. K. Heath, E. C. Nice and F. Caruso, *Adv. Mater.*, 2010, **22**, 5398.
6 P. Nagpal, N. C. Lindquist, S. H. Oh and D. J. Norris, *Science*, 2009, **325**, 594.
7 K. Okamoto, I. Niki, A. Shvartser, Y. Narukawa, T. Mukai and A. Scherer, *Nat. Mater.*, 2004, **3**, 601.
8 R. Bardhan, N. K. Grady and N. J. Halas, *Small*, 2008, **4**(10), 1716.
9 F. Tam, G. P. Goodrich, B. R. Johnson and N. J. Halas, *Nano Lett.*, 2007, **7**(2), 496.
10 T. S. Oh, H. Jeong, Y. S. Lee, J. D. Kim, T. H. Seo, H. Kim, A. H. Park, K. J. Lee and E. K. Suh, *Appl. Phys. Lett.*, 2009, **95**, 111112.
11 M. K. Kwon, J. Y. Kim, B. H. Kim, I. K. Park, C. Y. Cho, C. C. Byeon and S. J. Park, *Adv. Mater.*, 2008, **20**, 1253.
12 D. M. Yeh, C. Y. Chen, Y. C. Lu, C. F. Huang and C. C. Yang, *Nanotechnology*, 2007, **18**, 265402.
13 P. Benzo, L. Cattaneo, C. Farcau, A. Andreozzi, M. Perego, G. Benassayag, B. Pecassou, R. Carles and C. Bonafos, *J. Appl. Phys.*, 2011, **109**, 103524.
14 Y. Han, R. Lupitskyy, T. M. Chou, C. M. Stafford, H. Du and S. Sukhishvili, *Anal. Chem.*, 2011, **83**, 5873.
15 L. W. Jang, D. W. Jeon, T. Sahoo, D. S. Jo, J. W. Ju, S. J. Lee, J. H. Baek, J. K. Yang, J. H. Song, A. Y. Polyakov and I. H. Lee, *Opt. Express*, 2012, **20**(3), 2116.
16 L. W. Jang, T. Sahoo, D. W. Jeon, M. Kim, J. W. Jeon, D. S. Jo, M. K. Kim, Y. T. Yu, A. Y. Polyakov and I. H. Lee, *Appl. Phys. Lett.*, 2011, **99**, 251114.
17 L. W. Jang, D. W. Jeon, M. Kim, J. W. Jeon, A. Y. Polyakov, J. W. Ju, S. J. Lee, J. H. Baek, J. K. Yang and I. H. Lee, *Adv. Funct. Mater.*, 2012, **22**, 2728.
18 E. Dulkeith, T. Niedereichholz, T. A. Klar, J. Feldmann, G. V. Plessen, D. I. Gittins, K. S. Mayya and F. Caruso, *Phys. Rev. B: Condens. Matter Mater. Phys.*, 2004, **80**, 205424.
19 W. L. Barnes, *J. Opt. A: Pure Appl. Opt.*, 2006, **8**, S87.
20 N. C. Greenham, X. Peng and A. P. Alivisatos, *Phys. Rev. B: Condens. Matter*, 1996, **54**, 24.
21 F. Gao, Q. Lu and D. Zhao, *Nano Lett.*, 2003, **3**(1), 85.
22 P. Mulvaney, *Langmuir*, 1996, **12**, 788.
23 J. W. Liaw, *Eng. Anal. Boundary Elem.*, 2006, **30**, 734.
24 K. L. Kelly, E. Coronado, L. L. Zhao and G. C. Schatz, *J. Phys. Chem. B*, 2003, **107**, 668.
25 W. Wang, Z. Li, B. Gu, Z. Zhang and H. Xu, *ACS Nano*, 2009, **3**(11), 3493.
26 R. Bardhan, N. K. Grady, J. R. Cole, A. Joshi and N. J. Halas, *ACS Nano*, 2009, **3**(3), 744.
27 L. A. Kim, P. O. Anikeeva, S. A. Coe-Sullivan, J. S. Stechkel, M. G. Bawendi and V. Bulovic, *Nano Lett.*, 2008, **12**, 4513.
28 P. Andrew and W. L. Barnes, *Science*, 2004, **306**, 5.
29 S. Nizamoglu, B. elturk, D. W. Jeon, I. H. Lee and H. V. Demir, *Appl. Phys. Lett.*, 2011, **98**, 163108.
30 P. Anger, P. Bharadwaj and L. Novotny, *Phys. Rev. Lett.*, 2006, **96**, 113002.
31 W. Sigle, J. Nelayah, C. T. Koch and P. A. van Aken, *Opt. Lett.*, 2009, **34**, 14.
32 E. Dulkeith, A. C. Morteani, T. Niedereichholz, T. A. Klar, J. Feldmann, S. A. Levi, F. C. J. M. Van Veggel, D. N. Reinhoudt, M. Moller and D. I. Gittins, *Phys. Rev. Lett.*, 2002, **89**, 20.
33 Z. M. Sui, X. Chen, L. Y. Wang, L. M. Xu, W. C. Zhuang, Y. C. Chai and C. J. Yang, *Phys. E.*, 2006, **33**, 308.
34 M. Kawasaki and S. Mine, *J. Phys. Chem. B*, 2005, **109**, 17254.
35 R. F. Oulton, V. J. Sorger, T. Zentgraf, R. M. Ma, C. Gladden, L. Dai, G. Bartal and X. Zhang, *Nature*, 2009, **461**(1), 629.
36 In standard structures, the increase of the luminescence quantum yield is accompanied by the increase of the characteristic PL decay time. Because the radiative lifetime is more or less fixed by the material parameters and cannot be easily changed, this increase has to be achieved by increasing the non-radiative recombination lifetime, *i.e.* decreasing the density of non-radiative recombination centers by careful growth optimization. In contrast, in structures with LSP enhancement the LSP–MQW coupling creates a very fast alternative radiative recombination path. Therefore, in such structures, the increase in PL efficiency can occur together with a decrease in the effective PL relaxation time as has been widely reported (see, for example, ref. 7, 11 and 17).
37 D. W. Jeon, W. M. Choi, H. J. Shin, S. M. Yoon, J. Y. Choi, L. W. Jang and I. H. Lee, *J. Mater. Chem.*, 2011, **21**, 17688.
38 C. P. Liu and S. E. Wu, *Nanotechnology*, 2007, **18**, 445301.
39 K. Xu, J. X. Wang, X. L. Kang and J. F. Chen, *Mater. Lett.*, 2009, **63**, 31.
40 A. Mandal and N. Tamai, *J. Phys. Chem.*, 2008, **112**, 8244.
41 S. J. Byrne, S. A. Corr, T. Y. Rakovich, Y. K. Gun'ko, Y. P. Rakovich, J. F. Donegan, S. Mitchell and Y. Volkov, *J. Mater. Chem.*, 2006, **16**, 2896.
42 M. Gao, S. Kirstein, H. Mohwald, A. L. Rogach, A. Kornowski, A. Eychmuller and H. Weller, *J. Phys. Chem. B*, 1998, **102**, 8360.
43 J. Aldana, N. Lavelle, Y. Wang and X. Peng, *J. Am. Chem. Soc.*, 2005, **127**, 2496.
44 T. Ung, L. M. Liz-Marzan and P. Mulvaney, *Langmuir*, 1998, **14**, 3740.